

## Effect of Visible and UV Illumination on the Water Contact Angle of TiO<sub>2</sub> Thin Films with Incorporated Nitrogen

A. Borrás,<sup>†</sup> C. López,<sup>†</sup> V. Rico,<sup>†</sup> F. Gracia,<sup>†</sup> A. R. González-Elise,<sup>\*,‡</sup> E. Richter,<sup>‡</sup> G. Battiston,<sup>§</sup> R. Gerbasi,<sup>§</sup> N. McSporran,<sup>||</sup> G. Sauthier,<sup>||</sup> E. György,<sup>||</sup> and A. Figueras<sup>||</sup>

*Instituto de Ciencia de Materiales de Sevilla (CSIC-Univ. Sevilla), Avda, Américo Vespucio 49, 41092 Sevilla, Spain, Forschungszentrum Rossendorf, Institut für Ionenstrahlphysik und Materialforschung, P.O. Box 510119, 01314 Dresden, Germany, ICTIMA-CNR, Corso Stati Uniti 4, 35127 Padua, Italy, and ICMAB-CSIC, Campus de la UAB, 08193 Bellaterra, Spain*

*Received: August 21, 2006; In Final Form: November 13, 2006*

Doping TiO<sub>2</sub> with nitrogen is recognized as a procedure to get sensitization of this material with visible light. In the present work, incorporation of nitrogen within the structure of TiO<sub>2</sub> thin films has been accomplished by N<sub>2</sub><sup>+</sup> ion implantation in TiO<sub>2</sub> anatase thin films (50 keV ion energy for doses of  $3 \times 10^{16}$ ,  $6 \times 10^{16}$ , and  $1.2 \times 10^{17}$  ions cm<sup>-2</sup>) and during preparation by metalorganic chemical vapor deposition (MOCVD) using nitrogen as carrier gas. The analysis of the samples by X-ray photoemission spectroscopy (XPS) and for the MOCVD samples also by secondary ion mass spectroscopy (SIMS) has shown that nitrogen, in the form of nitride-like species, (N/Ti ratios of 0.03 and 0.12 for the MOCVD and the implanted samples, respectively) has become effectively incorporated within the structure of TiO<sub>2</sub>. The water contact angle on the implanted thin films varied from about 80° to around 30° when illuminated with visible light, depending on the ion dose. Similarly, the MOCVD samples showed a sharp decrease in wetting contact angle under visible light from about 80° to 55°. In the two cases, the thin films reach total hydrophilicity by posterior UV irradiation. To account for these results, the possible existence of specific excitation mechanisms for visible or UV photons, the former involving the incorporated nitrogen atoms, is discussed.

### Introduction

The activation of titanium oxide with light is a very interesting process with a large variety of applications, including the degradation of environmental pollutants in air and water, the recovery of metal cations from water, or the self-cleaning of glasses because of the modification of the wetting properties of its surface.<sup>1</sup> The wettability of materials is an important property in nature and technology.<sup>2</sup> Some years ago, Wang et al.<sup>3</sup> found that the surface of titanium dioxide thin films changed from hydrophobic to hydrophilic when subjected to UV irradiation. They also found that the normal contact angle of TiO<sub>2</sub> thin films (usually between 60° and 100°, depending on surface topography) was recovered when the films were illuminated with visible light or were stored in the dark, thus making reversible the change in wetting contact angle. Since this pioneering work, much effort has been dedicated to describe these UV-induced changes in hydrophilicity and to find the reasons for them.<sup>4–8</sup> At present, testing the wetting behavior of TiO<sub>2</sub> upon light irradiation is a common tool to check the photoactivity of this material.

The most widely accepted model of the wetting behavior of illuminated TiO<sub>2</sub> suggests that the photogenerated electron–hole pairs migrate to its surface where they induce a series of reactions leading to the hydroxylation of the surface, a feature that promotes its hydrophilic character. However, this view is

controversial and recently, Zubkov et al.,<sup>8</sup> after a careful experiment carried out in an ultrahigh vacuum equipment where the cleaning conditions can be effectively controlled, have attributed the changes in water contact angle to the photo-oxidative removal of the carbon contamination layer always present on the air-exposed surfaces of these oxides. Whatever the type of surface processes involved, it seems that the only effect of visible light on undoped TiO<sub>2</sub> is the acceleration in the recovery of the original hydrophobic character because of the thermal effects resulting from irradiation.<sup>7</sup>

The sensitization of TiO<sub>2</sub> with visible photons is a topic of the utmost interest<sup>9</sup> that has been induced by doping with transition-metal cations<sup>10–11</sup> or other atoms acting as anions.<sup>12</sup> In particular, Asahi et al.<sup>12</sup> have reported an improvement in the photocatalytic activity of TiO<sub>2</sub> doped with nitrogen, an effect confirmed by several other researchers.<sup>13–18</sup> It has been suggested that through both nitrogen doping and the presence of oxygen vacancies in its crystal structure, the activity of the TiO<sub>2</sub> photocatalyst in the visible region can be further enhanced.<sup>19–21</sup> Unfortunately, doping can also increase the number of electron–hole recombination centers and can reduce the thermal and mechanical stability of the material.<sup>22</sup> Addressing the wetting properties of TiO<sub>2</sub>, Premkumar<sup>16</sup> has reported that illumination with visible light of nitrogen-doped TiO<sub>2</sub> thin films prepared by magnetron sputtering results in the character of the material changing from hydrophobic to hydrophilic. This demonstrates that control of the wetting contact angle is possible without the assistance of UV photons. Some other recent investigations on TiO<sub>2</sub> thin films with incorporated nitrogen in their structure have also reported the possibility of inducing this change in water contact angle by illuminating with visible photons.<sup>23,24</sup>

\* Author to whom correspondence should be addressed. E-mail: arge@icmse.csic.es.

<sup>†</sup> Instituto de Ciencia de Materiales de Sevilla.

<sup>‡</sup> Institut für Ionenstrahlphysik und Materialforschung.

<sup>§</sup> ICTIMA-CNR.

<sup>||</sup> ICMAB-CSIC.

In the present paper, we report on the effect of visible light irradiation on the hydrophilicity of titanium oxide thin films where nitrogen has been incorporated in its structure by ion implantation or during their preparation by molecular organic chemical vapor deposition (MOCVD) using nitrogen as a carrier gas. The first procedure furnishes a precise control of the amount and distribution of incorporated nitrogen atoms. The second is an easily scalable method that is used for many industrial applications. A first aim of our work is to compare the wetting behavior of the two types of samples trying to get some information about the differences in light excitation processes with either visible or UV photons. The results obtained have shown that these two procedures are effective to incorporate nitrogen in the  $\text{TiO}_2$  structure and that the incorporated nitrogen atoms open new excitation channels that can be activated by visible light illumination. The possibility of obtaining intermediate values of water contact angles of nitrogen-doped  $\text{TiO}_2$  by illumination with visible light is discussed.

## Experimental Section

Samples were produced using MOCVD at 400 °C under a reactor pressure of 50 Pa as described elsewhere<sup>25</sup> (these samples will be called here MOCVD- $\text{TiO}_2$ ). Titanium tetraisopropoxide was used as Ti precursor. Nitrogen was used as carrier gas with a flow rate of 50  $\text{cm}^3/\text{min}$  and at the reactor entrance an additional flux of 10  $\text{cm}^3/\text{min}$  of oxygen was added. The constant growth rate was evaluated in 19  $\text{nm}/\text{min}$ . For comparison, some  $\text{TiO}_2$  samples were also grown under the same conditions but using Ar as carrier gas instead of  $\text{N}_2$ . However, these samples presented a slightly bluish color likely because of the presence of some  $\text{Ti}^{3+}$  species. Because of that, for most essays we use as a reference sample a fully stoichiometric  $\text{TiO}_2$  film prepared by plasma-enhanced chemical vapor deposition (PECVD). Typical thickness of the MOCVD samples was around 350 nm. Nitrogen ion implantation was carried out on  $\text{TiO}_2$  thin films with a similar thickness prepared by PECVD according to a procedure described in ref 26. Titanium tetraisopropoxide was used as Ti precursor and oxygen at a pressure of  $10^{-1}$  Torr was used as the sole plasma gas. Temperature of the substrate during deposition was 250 °C. These PECVD samples were fully stoichiometric and did not undergo any change in water contact angle when illuminated with visible light. The crystalline structure of all films determined by X-ray diffraction was polycrystalline anatase. The PECVD samples before ion implantation will be named as ref- $\text{TiO}_2$ .

Implantation of nitrogen with 50 keV  $\text{N}_2^+$  ions (ion doses of  $3 \times 10^{16}$ ,  $6 \times 10^{16}$ , and  $1.2 \times 10^{17}$  atoms  $\text{cm}^{-2}$ ) was carried out on the PECVD samples (the implanted samples will hereafter be called I- $\text{TiO}_2$ ). The implantation experiments were carried out with the high current ion implanter DANFYS 1090-200 (DANFYSIK A/S, Jyllinge Denmark) at the Institute of Ion Beam Physics and Materials Research in the Forschungszentrum Rossendorf, Germany. The maximum acceleration voltage of this machine is 200 kV. The ion beam is mass separated using a magnetic field. The beam current for  $\text{N}_2^+$  ions is in the range of a few mA. SRIM calculations<sup>27</sup> of the nitrogen distribution in these samples showed that the nitrogen extends according to a Gaussian-type profile over a thickness of about 200 nm with a relatively small concentration at the surface and a maximum at  $\sim 100$  nm for the films with the maximum dose of irradiation. Small variations around these values are obtained depending on the actual ion dose utilized. For simplicity, most characterization results reported in this work refer to the sample with a dose of  $1.2 \times 10^{17}$  atoms  $\text{cm}^{-2}$ .

Chemical analysis of films has been carried out by means of X-ray photoemission spectroscopy (XPS) and for the MOCVD- $\text{TiO}_2$  films also by secondary ion mass spectrometry (SIMS). The samples were also analyzed by XPS after sputtering with  $\text{Ar}^+$  ions of 1000 eV kinetic energy for increasing periods of time. For the ion dose utilized for the sputtering, an erosion rate of approximately 2  $\text{nm min}^{-1}$  can be estimated.

SIMS analysis of the MOCVD- $\text{TiO}_2$  films was carried out on a time-of-flight (TOF)-SIMS IV instrument from Ion-ToF GmbH Germany. The samples were bombarded with a pulsed gallium ion beam. The secondary ions generated were extracted with a 10 KV voltage and their time-of-flight from the sample to the detector was measured in a reflectron mass spectrometer. Typical analysis conditions for this work were 25 keV pulsed  $\text{Ga}^+$  beam at 45° incidence, rastered over  $150 \times 150$   $\mu\text{m}$ . Depth profile experiments used an additional dual beam  $\text{Cs}^+$  Ion Gun at 2 keV rastered over  $300 \times 300$   $\mu\text{m}$ . Electron flood gun charge compensation was necessary during measurements.

XPS spectra of MOCVD- $\text{TiO}_2$  and I- $\text{TiO}_2$  samples were recorded in a Vacuum Generator ESCALAB 210 spectrometer working in the constant band-pass energy mode at 50 eV. The Mg K $\alpha$  radiation was used as excitation source, and the binding energy (BE) scale was referred to the C 1s peak of the carbon contaminating the surface of samples at a value of 284.6 eV.  $\text{Ar}^+$  sputtering was done in the same spectrometer by bombarding with  $\text{Ar}^+$  ions of 3 keV kinetic energy. Since prolonged ion bombardment of oxides may produce some chemical changes, the sputtering time was limited to short periods just to show the existence of a certain evolution in depth of the N 1s intensity in the I- $\text{TiO}_2$  samples.

Water contact angle experiments were carried out after illumination for increasing periods of time. A 125 W Xe lamp (CERMAX PE175BUV from CVI) was used for these experiments. The light power of the lamp was calibrated by means of a silicon photodiode for photon detection (Spectra Physics model 407A). The maximum photon flux (i.e., UV + visible photons and the contribution from the IR part of the spectrum) measured at the sample position was 1.35  $\text{W cm}^{-2}$ . From this total intensity, 77% corresponded to the visible plus some near-IR contribution and 23% corresponded to the UV part. For simplicity, when presenting the results we will refer as "visible" the whole spectral region eliminating the UV portion of the spectrum. A F63 filter with a cutting edge at 420 nm was used for this calibration. Meanwhile, for the experiments where we examined the changes in wetting contact angles upon visible light illumination, we used as a filter a polymer plate with a cutting edge at 380 nm.

For some experiments, lamp intensity was adjusted by means of an output diaphragm that also acted as output slit. The terms "low", "medium", and "high" intensity used in the work correspond to full spectrum intensities of 0.02, 0.4, and 1.35  $\text{W cm}^{-2}$ . However, since modifying the output slit may also modify the spectral distribution, the results obtained with different intensities of light will not be considered to make any quantitative correlation but just to show tendencies in the kinetic changes of the water contact angles on  $\text{TiO}_2$  under illumination.

Measurement of contact angle was carried out by dosing small droplets of water on the surface of the illuminated samples. Curves describing the change in the contact angle versus irradiation time for MOCVD- $\text{TiO}_2$  and I- $\text{TiO}_2$  samples were carried out for different light powers or by selecting the visible part of the spectrum. In the experiments where the contact angle variation was determined as a function of the illumination time, a metal foil acting as a shutter was used to close and open the

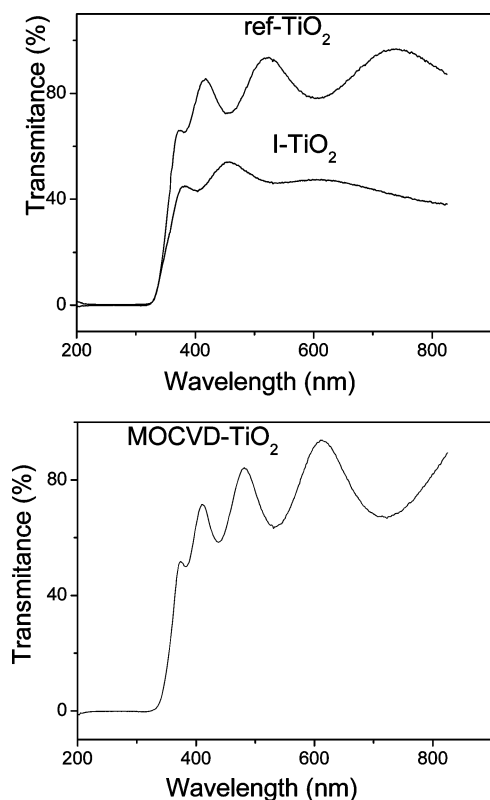


**Figure 1.** (top) UV-vis absorption spectra of the I-TiO<sub>2</sub> sample ( $1.2 \times 10^{17}$  atoms cm<sup>-2</sup>) as compared with the spectrum of the same sample before implantation (sample ref-TiO<sub>2</sub>). (bottom) UV-vis absorption spectrum of the MOCVD sample.

lamp output. All wetting angle measurements within a given experiment were taken after illumination for successive periods of time. The time scale in the plots refers to the accumulative illumination of the samples. The uncertainty in the determination of the water contact angle is about  $\pm 5^\circ$  depending on the sample position. Some variation curves of contact angles were fitted with exponential curves. From these curves, the kinetic constants ( $k$ ) are estimated by normalizing with the value of the light intensity (visible or UV) assumed to be active in each case.

## Results

**UV-Vis Spectra and Surface Topography of I-TiO<sub>2</sub> and MOCVD Samples.** It is generally accepted that N incorporation in the lattice of TiO<sub>2</sub> changes the absorption spectrum of this material by generating electronic states in the band gap that can be excited with visible light.<sup>12,16,28</sup> Figure 1 shows the UV-vis absorption spectra of PECVD samples before (i.e., sample ref-TiO<sub>2</sub>) and after implantation (i.e., sample I-TiO<sub>2</sub>) and that of the MOCVD sample. These spectra are characterized by oscillations in transmittance appearing because of the different refraction index of the substrate and layers. Neither in the

I-TiO<sub>2</sub> nor in the MOCVD-TiO<sub>2</sub> samples is there any significant shift in the absorption edge if compared with that of ref-TiO<sub>2</sub>. This means that no narrowing of the band gap occurs because of the implantation of nitrogen in I-TiO<sub>2</sub> samples or during the preparation of MOCVD-TiO<sub>2</sub> samples. By comparing the spectra of the I-TiO<sub>2</sub> and ref-TiO<sub>2</sub> samples, it is apparent that the main effect of nitrogen implantation in the former case is a general drop in the transmittance of the films in the whole spectral region. Visually, this drop produces a brown color in a sample that is still partially transparent. A similar, though smaller, drop in transmittance can be appreciated in the MOCVD-TiO<sub>2</sub> films, particularly for  $\lambda > 500$  nm. In this sample, no color could be clearly appreciated by visual inspection. The observed decrease in transmittance can be associated with the incorporation of nitrogen into the TiO<sub>2</sub> lattice, although other factors like surface layer roughening or other related modifications of the optical properties of the films because of the generation of defects (e.g., oxygen vacancies<sup>29</sup>) might also contribute to it. The formation of oxygen vacancies is very likely to occur in the I-TiO<sub>2</sub> samples owing to the high energy of the nitrogen ions used for implantation. Modifications of the surface topography upon ion implantation are in fact evidenced by Figure 2 showing the atomic force microscopy (AFM) images of the ref-TiO<sub>2</sub> sample before and after ion implantation with a dose of  $1.2 \times 10^{17}$  ions cm<sup>-2</sup>. According to these two images, it is clear that the surface topography of the I-TiO<sub>2</sub> sample has been significantly altered, now presenting a rougher topography characterized by broader and bigger surface aggregates. On the other hand, the surface topography of the MOCVD-TiO<sub>2</sub> samples is characterized by smaller surface oscillations and less roughness. This is congruent with the fact that this sample is heated at 400 °C during preparation, likely leading to diffusion, reconstructions, and sintering processes that flatten the surface.

### Detection of N in the MOCVD-TiO<sub>2</sub> and I-TiO<sub>2</sub> Samples.

A tentative explanation of the changes in water contact angles upon visible light illumination that are reported in the next sections is based on the assumption that nitrogen incorporated in the lattice of TiO<sub>2</sub> produces new electronic states in the gap that can be excited with photons of a wavelength longer than that corresponding to the band gap of TiO<sub>2</sub>. A requisite for such an explanation is that nitrogen is effectively incorporated in the samples. In the case of MOCVD-TiO<sub>2</sub> thin films, we assume that nitrogen incorporates in the films because of the use of this gas as carrier gas during their synthesis. This assumption was confirmed by SIMS analysis showing the evolution of the TiNOH<sub>2</sub> fragment (atomic mass 80) during ion bombardment. This fragment cannot be produced by any other ensemble of atoms coming from the film and therefore must be the result of the incorporation of nitrogen into its structure during its synthesis by MOCVD. The mass spectrometer resolution is high enough for discriminating this peak of the associated to TiO<sub>2</sub>. In consequence, it is a very good fingerprint for N detection. No

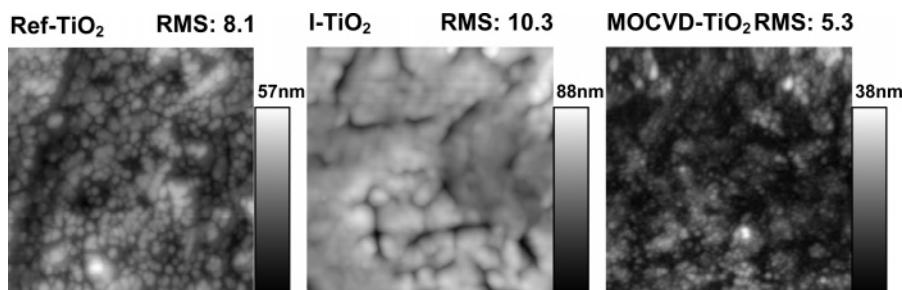


**Figure 2.** AFM images of the ref-TiO<sub>2</sub> (left), I-TiO<sub>2</sub> (middle), and (right) MOCVD-TiO<sub>2</sub> thin films.



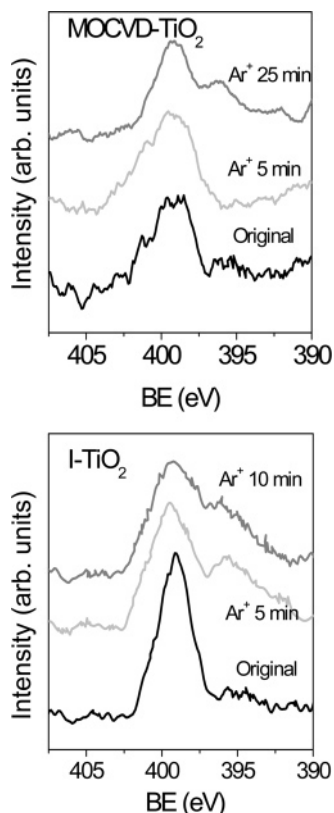


**Figure 3.** N 1s photoemission spectra of samples MOCVD-TiO<sub>2</sub> (top) and I-TiO<sub>2</sub> (bottom) subjected to Ar<sup>+</sup> sputtering for increasing periods of time.

fragments of this kind were detected for ref-TiO<sub>2</sub> or MOCVD samples prepared with Ar as carrier gas. In addition, as reported in Figure 3, XPS analysis of MOCVD-TiO<sub>2</sub> samples showed N 1s photoemission peaks located approximately at 396 and 400 eV, corresponding to different environments between Ti-N and Ti-N(O) with a variable number of Ti-N and Ti-O bonds.<sup>23,28,30–32</sup> It is interesting by this analysis that these nitrogen species distribute through all the film thickness as they appear even after Ar<sup>+</sup> sputtering of the samples for prolonged periods of time. From all these data, an estimation of the nitrogen concentration in the film yielded values around 0.03 atoms of nitrogen per atom of titanium in the nonsputtered sample.

For the I-TiO<sub>2</sub> samples, the results of a similar XPS analysis showed the presence of similar species of nitrogen. The N 1s photoemission spectra of this sample reported in Figure 3 are characterized by two main peaks located at about 396 and 400 eV, also attributed to nitrogen in different Ti-N/Ti-N(O)

environments.<sup>23,28,30–32</sup> In the present case, the relative concentration of nitrogen with respect to Ti was of 0.12 atoms per atom of titanium for the sample implanted with the highest ion dose. This ratio, obtained for the nonsputtered sample, increased after a mild sputtering for 10 min as expected for the first part of the profile calculated with the SRIM code,<sup>27</sup> consisting of a Gaussian type profile with a maximum located at around 100 nm from surface.

**Contact Angle on Thin Films Illuminated with Visible Light.** The initial contact angle of the different films was about 80°. Although the films were carefully cleaned before their analysis, it cannot be discarded that some contribution to this relatively high contact angle is due to the presence of some organic contamination on their surface. The evolution of the water contact angle for the I-TiO<sub>2</sub> films was investigated upon visible light illumination. Figure 4 shows the evolution of the contact angle of the three I-TiO<sub>2</sub> thin films subjected to visible light illumination for increasing periods of time. It is apparent that after irradiation for a short period of time (~two-thirds of a minute) the water contact angle of the sample with  $1.2 \times 10^{17}$  ions decreased from ~80 to ~30°, remaining at this value after prolonged illumination for more than 40 min (i.e., steady-state values). For the other two I-TiO<sub>2</sub> thin films, similar curves were obtained, although in this case the contact angles at the steady state were ~45° (film with  $6 \times 10^{16}$  atoms cm<sup>-2</sup>) and ~30° (film with  $3 \times 10^{16}$  atoms cm<sup>-2</sup>), and steady values were reached after illumination for ~2 and ~14 min, respectively. For these three samples, a posterior illumination with the full spectrum of the Xe lamp brought the wetting angle to a value smaller than 10° (i.e., total hydrophilicity). No change in this state was observed when the samples were illuminated again with visible light (curves not shown for simplicity).

The evolution of the contact angle for the MOCVD-TiO<sub>2</sub> sample illuminated with visible and UV + visible light is reported in Figure 5. The plot in this figure clearly shows a sharp and well-defined decrease in contact angle from 80° to around 55° when this sample is illuminated with visible light. However, once this value of 55° was reached, the contact angle remained constant irrespective of the irradiation time (50 min in the experiment shown in Figure 5a). This result confirmed that, similarly as for the I-TiO<sub>2</sub> samples (cf. Figure 4), in the MOCVD-TiO<sub>2</sub> films visible photons are able to induce some surface photochemical processes leading to a partial decrease in contact angle. After this first decay, the UV filter was removed and the film was exposed to full spectrum illumination with the low intensity of the lamp. This action resulted in a further decrease of contact angle, the surface becoming fully hydrophilic. Furthermore, once the hydrophilic character of this

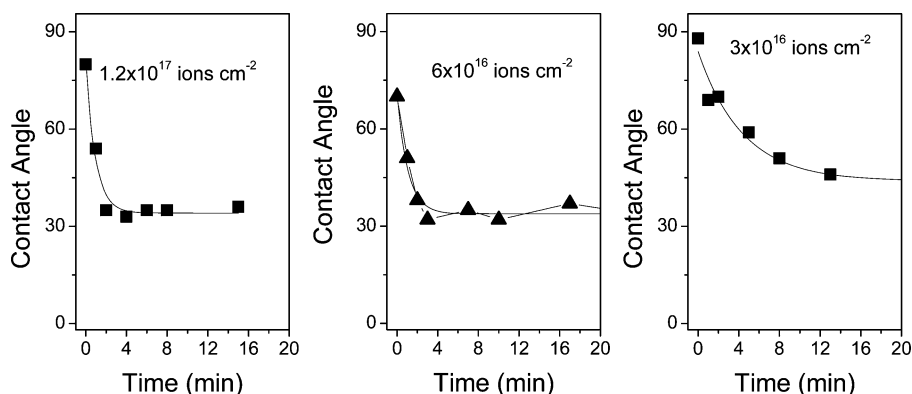


**Figure 4.** Evolution of the water contact angle for the I-TiO<sub>2</sub> thin films illuminated with visible light. From left to right the panels show the curves corresponding to a decreasing amount of implanted nitrogen ions. The continuous curves are fitting exponentials.

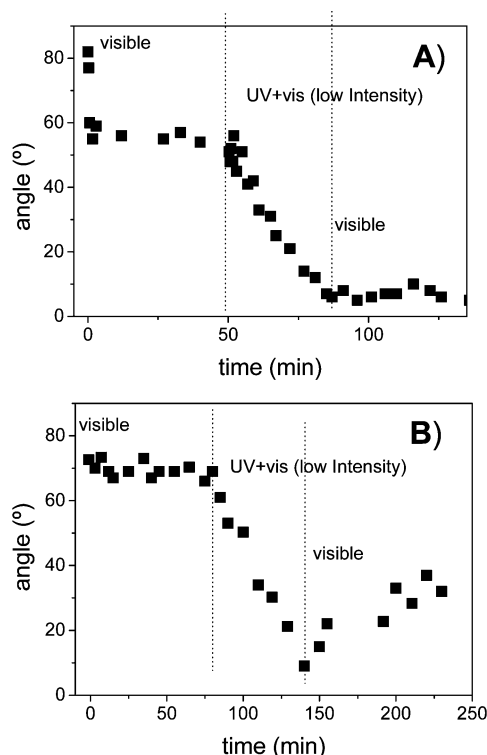


**Figure 5.** Evolution of the water contact angle for the MOCVD (A) and ref-TiO<sub>2</sub> (B) samples subjected to sequential illumination with visible, (UV + vis), and visible photons.

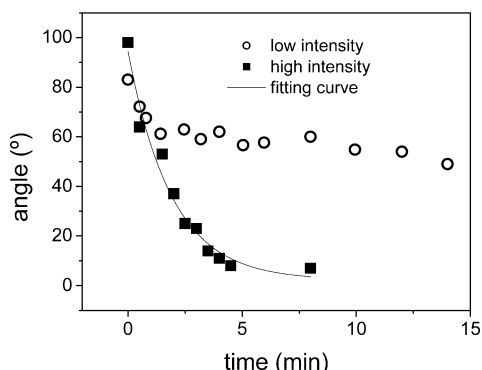


**Figure 6.** Evolution of the water contact angles of ref-TiO<sub>2</sub> thin film illuminated with different intensities of the full spectrum of the Xe lamps. An exponential curve fitting the experimental points obtained with the maximum intensity of the lamp is also included in the figure.

sample was obtained, it remained in this state even after illumination with visible light for a prolonged period of time. This is a different behavior than that of TiO<sub>2</sub> films referenced in the literature<sup>3–7</sup> and that of the ref-TiO<sub>2</sub> films studied here. Thus, Figure 5b confirms that irradiation with visible light of a ref-TiO<sub>2</sub> film did not produce any significant decrease in contact angle, while under UV light the sample became fully hydrophilic. Moreover, unlike the MOCVD–TiO<sub>2</sub> sample, when the ref-TiO<sub>2</sub> sample was subsequently illuminated with visible light, a recovery of contact angle was observed.

**Contact Angles on TiO<sub>2</sub> Thin Films Illuminated with UV + Visible Light.** Following the known behavior of TiO<sub>2</sub>, UV + vis irradiation of ref-TiO<sub>2</sub> sample induced a drastic decrease in the water contact angle to a value smaller than 10° (i.e., complete hydrophilicity) after illumination for about 5 min (Figure 6). The kinetics of this process was very sensitive to the intensity of illumination and the rate decreased when the experiment was conducted with the “low” intensity of the lamp.

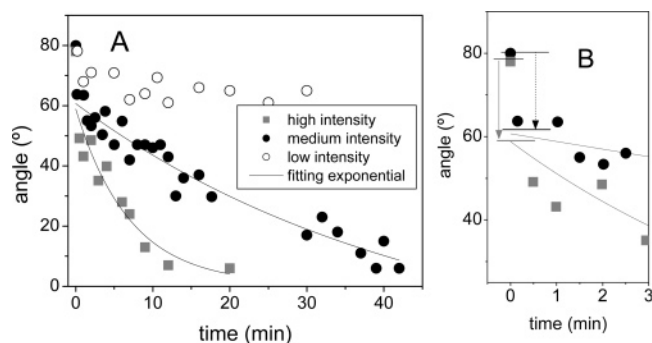


**Figure 7.** (A) Evolution of the water contact angles of MOCVD–TiO<sub>2</sub> thin films illuminated with different intensities of the full spectrum of the Xe lamps. Exponential curves that fit the experimental points are also included in the figure. (B) The right-hand panel shows in an enlarged scale the initial points of the experiments for high and medium lamp intensities.

The water contact angle recovered after prolonged storage of this unimplanted film in the dark or by visible light illumination. The recovery was accelerated when the sample was kept at about 100 °C. This is the normal behavior reported for stoichiometric TiO<sub>2</sub>.<sup>3–8</sup>

In another experiment, MOCVD samples were first irradiated with the full spectrum of the Xe lamp, and the evolution of the contact angle as a function of the irradiation time is shown in Figure 7. In this case, the effect of low, medium, and high lamp intensities is reported. It is clear from the figure that curve profiles were strongly dependent on light intensity and that lower light intensities gave rise to slower contact angle decays. This behavior indicates that the change in contact angle is limited by the number of electron–hole pairs produced by light irradiation. The results obtained for high and medium intensities show a sharp decay in contact angle from 80° to around 60°, followed by a smoother decrease up to total hydrophilicity (see the right-hand side panel in Figure 7 for the illumination with both high and medium intensities of the lamp). This behavior suggests the superposition of two independent processes characterized by two different kinetics.

This behavior is different than that found for stoichiometric TiO<sub>2</sub>, as can be seen by comparison of these results with those in Figure 6 corresponding to the decrease of contact angle for a stoichiometric ref-TiO<sub>2</sub>. For this sample, the variation in contact angle follows a single profile, where the minimum contact angle is reached after a relatively shorter period of time.

The illuminated MOCVD–TiO<sub>2</sub> films studied in this section recovered a contact angle of ~60° by storing in the dark for several hours. Keeping the samples in air at around 100 °C led to a full recovery of contact angle (i.e., 80°) in a matter of tens of minutes.

## Discussion

In general, the initial contact angle of the different samples studied here is rather large. A combination of contributions due to the presence of some carbonaceous contamination or the roughness of the films might be the reason for such an effect. After illumination, this contact angle decreases by a different amount depending on the type of sample and the wavelengths of light.

The change in contact angle observed for MOCVD–TiO<sub>2</sub> samples when irradiated with the total spectrum of light of the lamp (i.e., visible + UV photons, Figure 7) depicts a first sharp decrease followed by a second smoother decrease. This evolution suggests the existence of two independent processes. The

kinetics of contact angle decay when a TiO<sub>2</sub> thin film is irradiated with UV photons has been studied by many authors.<sup>4–7</sup> It has been also confirmed by other authors that the water contact angle conversion proceeds faster at higher light intensities.<sup>33,34</sup> According to Ralston,<sup>5</sup> the kinetics of the contact angle decay can be described using an exponential expression:

$$\Theta = \theta_0 \exp(-k_p t)$$

By fitting the curves for I–TiO<sub>2</sub>, ref-TiO<sub>2</sub>, and MOCVD–TiO<sub>2</sub> samples in Figures 4, 6, and 7 with a similar exponential decay function, it is possible to get a set of values for the kinetic constants  $k_p$  of the decay process. For the MOCVD–TiO<sub>2</sub> films, the initial contact angle decay from about 80° to 55° in Figure 7 cannot be fitted with the same curve as for the other points of the experiment. This suggests that this initial decay follows a different mechanism characterized by a different decay function. The obtained kinetic constants  $k_p$  have been normalized with the intensity of light (UV, visible, or UV + visible) which is assumed to be active in modifying the contact angle for each sample. The obtained  $k$  values, corrected by the actual intensity of light and therefore expressed in units of min<sup>–1</sup> W<sup>–1</sup>, were as follows for the different analyzed kinetics:

(a) MOCVD–TiO<sub>2</sub> sample, irradiation with visible light inducing a decrease in contact angle from about 80° to 55° (cf. Figure 5a and first decay in Figure 7) 1.44 min<sup>–1</sup> W<sup>–1</sup>.

(b) MOCVD–TiO<sub>2</sub> sample, irradiation with UV + visible photons, but assuming that only the UV intensity is effective in decreasing contact angle in the part where an exponential curve is fitted (cf. exponential curve in Figure 7) 0.355 min<sup>–1</sup> W<sup>–1</sup>.

(c) ref-TiO<sub>2</sub> sample, irradiation with UV + visible photons, but assuming that only UV power is effective in decreasing contact angle from 80° to 0° (cf. Figure 6) 1.315 min<sup>–1</sup> W<sup>–1</sup>.

(d) I–TiO<sub>2</sub> samples, illumination with visible light (cf. Figure 4) 2.49, 0.61, and 0.54 min<sup>–1</sup> W<sup>–1</sup> for the samples with  $1.2 \times 10^{17}$ ,  $6 \times 10^{16}$ , and  $3 \times 10^{16}$  atoms cm<sup>–2</sup>. For these samples, the contact angle decreased from approximately 80°, 65°, and 90° before illumination to 30°, 30°, and 45° after illumination.

In relation with the previous data, it must be mentioned that the calculated  $k$  values estimated for visible light illumination are actually the smallest limit of these constant since they are normalized by the total intensity of visible (plus near IR) light. This is so because from all this light intensity, the portion corresponding to long-wavelength photons are very likely inactive in inducing the hydrophilic transformation. Although these values must only be considered as having a semiquantitative meaning, it is interesting that the lowest-limit  $k$  values found for the visible excitation of the MOCVD–TiO<sub>2</sub> films are higher than the value found for this sample irradiated with UV photons. This difference indicates that the photon yield for visible light irradiation of these samples is higher than that for UV photons. Another interesting feature is that visible light irradiation does not bring the surface to a zero contact angle but to an intermediate steady-state value. Very recently, we have found a similar behavior for illuminated ZnO and InTa<sub>2</sub>O<sub>5</sub> thin films and have attributed it to the existence of intrinsic electronic defects in their electronic structure.<sup>35</sup>

The results with the I–TiO<sub>2</sub> samples illuminated with visible light may provide additional clues to account for the behavior of N-doped samples. A first evidence is that for the sample with the maximum dose of implanted nitrogen (i.e.,  $1.2 \times 10^{17}$  ions cm<sup>–2</sup>) the kinetic constant for visible light illumination (i.e., 2.49 min<sup>–1</sup> W<sup>–1</sup>) is higher than that of the ref-TiO<sub>2</sub> excited with UV + vis photons (i.e., 1.315 min<sup>–1</sup> W<sup>–1</sup>). We think that the

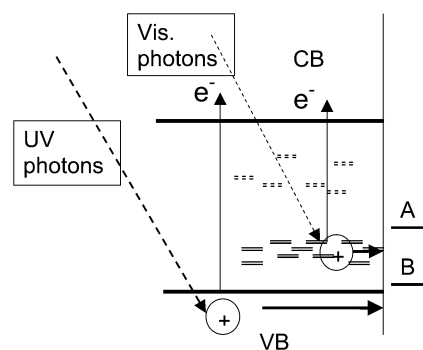


**Figure 8.** Scheme to account for the effect of visible light in the N-doped samples. The electronic states formed in the gap close to the valence band are attributed to N 2p states. The holes produced by visible light excitation of these states have enough energy as to induce a reaction involving the surface states A but not to do it with states B. In this case, only a partial hydrophilicity can be induced with visible photons. The holes produced in the valence band by UV irradiation have enough energy as to induce surface reactions involving both types of states A and B, thus bringing the surface to complete hydrophilicity. Band bending is not considered in the plot for simplicity.

fast kinetics found for the N-doped sample with the maximum dose of nitrogen and the fact that total hydrophilicity is not reached when any of the I–TiO<sub>2</sub> samples are illuminated with visible light can be explained by assuming the energy scheme in Figure 8. According to recent theoretical calculations of Lee et al.,<sup>36</sup> the incorporation of nitrogen ions within the lattice of TiO<sub>2</sub> produces the generation of a series of N 2p electronic states in the gap near the valence band, while no band gap narrowing takes place. The scheme in Figure 8 represents such a situation for the N-doped TiO<sub>2</sub> where, as a result of the incorporation of nitrogen within the structure, electronic states have been formed in the gap close to the valence band. Eventually, some oxygen vacancies produced during the ion implantation process or during the synthesis of the MOCVD samples could also lead to the generation of other electronic defects. In this case, the associated states can be distributed through the entire band gap, thus accounting for by the general decrease in transmittance observed for the I–TiO<sub>2</sub> films (i.e., darkening, see Figure 1). This situation is particularly likely by ion implantation, a nonequilibrium process that might lead to the generation of a relatively large dispersion of energies for the electronic defects associated to oxygen vacancies. Electronic excitations by visible light illumination of the N-associated electronic states would produce electron–hole pairs responsible to induce the surface reactions that convert the surface of TiO<sub>2</sub> to hydrophilic. Whether these reactions involve processes converting tiloxane (i.e., Ti–O–Ti) into tilanol (i.e., Ti–OH) surface groups, as first assumed,<sup>4–8</sup> or involve the partial or total removal by oxidation of a carbonaceous contaminating layer in line with the proposal by Zubkov et al.<sup>8</sup> does not alter these arguments. For these electron–hole pairs produced by visible photons, the energy of the holes, responsible for initiating the photochemical reactions at the surface, will be lower than for the holes produced in the valence band by UV irradiation (see the scheme in Figure 8). If this is the case, our wetting angle results suggest that transformation of the TiO<sub>2</sub> surface into its hydrophilic state implies a series of differently energy-demanding reactions involving different surface species (denoted by A and B in the scheme of Figure 8). Thus, the holes produced with visible photons would only be able to induce a partial surface transformation by reacting with species A, while other surface species like B would remain unaffected by them. According to the scheme of Figure 8, species B would only react when a



hole produced in the valence band reaches the surface. The fact that the steady-state angle is smaller in the I–TiO<sub>2</sub> than in the MOCVD–TiO<sub>2</sub> thin films would be in agreement with the fact that in the former case a broader energy distribution is expected for the N-induced electronic states (and therefore for the energy of the photogenerated holes) produced by ion implantation. This idea is also confirmed by the different behavior found for the three different implanted samples where the steady-state angle depends on the implantation dose with a saturation response for a dose of  $6 \times 10^6$  ions cm<sup>-2</sup>. A similar model has been recently proposed by Nakamura et al.<sup>37</sup> who reported an enhancement in the photochemical oxidation of some compounds like I<sup>-</sup> and hydroquinone when N-doped TiO<sub>2</sub> is illuminated with visible light, while no enhancement is found for other compounds like SCN<sup>-</sup> or Br<sup>-</sup>. These authors assume that the electrochemical potential associated to I<sup>-</sup> and hydroquinone are situated in the gap as proposed for species A in our case, while SCN<sup>-</sup> and Br<sup>-</sup> will be characterized by an electrochemical potential situated close to the valence band edge as it happens for our species B. This model is somehow contradictory with the recent proposal by Irie et al.<sup>38</sup> that assumes some band gap narrowing to explain the hydrophilic conversion by visible light illumination of a N-doped TiO<sub>2</sub> thin film prepared by magnetron sputtering. The simultaneous formation of oxygen vacancies together with nitrogen incorporation might be one of the differential features for our working conditions in comparison with those of these authors.

Within the previous scheme, we do not have yet a sustained explanation for the observation of a faster kinetics when the surface processes are induced by visible photons than with UV photons. A possibility would be that electron–hole recombination processes before arriving to the surface are more likely for the UV-induced excitons (e–h<sup>+</sup> pair). In a previous theoretical model to account for the visible light activity of defective titanium oxide with a high concentration of oxygen vacancies, we have proposed the formation of a continuous “miniband” of electronic states<sup>29</sup> in the gap. A similar overlapping of N 2p electronic levels, particularly important for the I–TiO<sub>2</sub> sample, with the maximum concentration of implanted nitrogen could produce a kind of continuous band where the mobility of holes, and therefore the rate of conversion into the hydrophilic state, would be enhanced. This effect should largely overcome the increase in the electron–hole recombination favored by the structural damage in the surface induced in these materials by the implantation process (see the AFM images in Figure 2).

## Conclusions

The experiments discussed in the previous sections have revealed that nitrogen in the form of nitride-like species can be incorporated within the structure of TiO<sub>2</sub> during its preparation by MOCVD and by ion implantation with an ion accelerator. In the latter case, some surface damage and an extra generation of electronic defects are induced as shown, respectively, by AFM and UV–vis absorption. A common behavior of the TiO<sub>2</sub> thin films with incorporated nitrogen is that they change their water contact angle when illuminated with visible light. The generation of electronic states in the gap associated to the nitride species is a likely factor determining the visible light excitation processes. In this regard, the final steady-state value of the contact angle reached by visible illumination seems to depend on the type or amount of electronic states generated by the incorporated nitrogen and hence on the method used to prepare the N-doped thin films.

Another interesting piece of evidence is that, for a given sample, the kinetics of water contact angle variation when the

samples are illuminated with visible light uses to be faster than that of the processes induced with UV photons. Although there is not yet a clear view of the reasons for this behavior, it seems apparent that this different kinetics behavior indicates the existence of different excitation channels for visible or UV photons.

**Acknowledgment.** This paper is dedicated to the memory of G. Battiston. This work has been partially supported by bilateral programmes of cooperation between CSIC–CNR as well as the contract number 2001SGR00333(Dursi) and Department de Medi Ambient i Habitatge de la Generalitat de Catalunya. We acknowledge Dr. C. Serra for his help in SIMS measurements. The contribution of the Spanish Ministry for Science and Education (project MAT2004-01558) and CSIC (project PIF– 200460F0230) is also acknowledged. We also thank the Forschungszentrum Rossendorf for the implantation of the I–TiO<sub>2</sub> samples.

## References and Notes

- (1) Carp, O.; Huisman, C. L.; Reller, A. *Prog. Solid State Chem.* **2004**, 32, 33.
- (2) Blossey, R. *Nat. Mater.* **2003**, 2, 301.
- (3) Wang, R.; Hashimoto, K.; Fujishima, A.; Chinkuni, M.; Kojima, E.; Kitamura, A.; Shimohigoshi, M.; Watanabe, T. *Nature* **1997**, 388, 432.
- (4) Watanabe, T.; Nakajima, A.; Wang, R.; Minabe, M.; Koizumi, S.; Fujishima, A.; Hashimoto, K. *Thin Solid Films* **1999**, 351, 260.
- (5) Stevens, N.; Priest, C. I.; Sedev, R.; Ralston, J. *Langmuir* **2003**, 19, 3272.
- (6) Zeman, P.; Takabayashi, S. *J. Vac. Sci. Technol.* **2002**, 20, 388.
- (7) Miyauchi, M.; Kieda, N.; Hishita, Sh.; Mitsuhashi, T.; Nakajima, A.; Watanabe, T.; Hashimoto, K. *Surf. Sci.* **2002**, 511, 401.
- (8) Zubkov, T.; Stahl, D.; Thompson, T. L.; Panayotov, D.; Diwald, O.; Yates, J. T. *J. Phys. Chem. B* **2005**, 109, 15454.
- (9) Carp, O.; Huisman, C. L.; Reller, A. *Prog. Solid State Chem.* **2004**, 32, 33.
- (10) Anpo, M.; Takeuchi, M. *J. Catal.* **2003**, 216, 505.
- (11) Gracia, F.; Holgado, J. P.; Caballero, A.; González-Elipe, A. R. *J. Phys. Chem. B* **2004**, 108, 17466.
- (12) Asahi, R.; Morikawa, T.; Ohwaki, T.; Aoki, K.; Taga, Y. *Science* **2001**, 293 (5528), 269.
- (13) Ihara, T.; Miyoshi, M.; Iriyama, Y.; Matsumoto, O.; Sugihara, S. *Appl. Catal., B* **2003**, 42, 403.
- (14) Wei, H.; Wu, Y.; Lun, N.; Zhao, F. *J. Mater. Sci.* **2004**, 39, 1305.
- (15) Suda, Y.; Kawasaki, H.; Ueda, T.; Ohshima, T. *Thin Solid Films* **2004**, 453, 162.
- (16) Premkumar, J. *Chem. Mater.* **2004**, 16, 3980.
- (17) Nosaka, Y.; Matsushita, M.; Nishino, L.; Nosaka, A. Y. *Sci. Tech. Adv. Mater.* **2005**, 6, 143.
- (18) Wang, Z.; Cai, W.; Hong, X.; Zhao, X.; Xu, F.; Cai, C. *Appl. Catal., B* **2005**, 57, 223.
- (19) Sakthivel, S.; Janczarek, M.; Kisch, H. *J. Phys. Chem. B* **2004**, 108, 19384.
- (20) Di Valentin, C.; Pacchioni, G.; Selloni, A.; Livraghi, S.; Giamello, E. *J. Phys. Chem. B* **2005**, 109, 11414.
- (21) Pan, X.; Ma, X. *J. Solid State Chem.* **2004**, 177, 4098.
- (22) Choi, W. Y.; Termin, A.; Hoffmann, M. R. *J. Phys. Chem.* **1994**, 98, 13669.
- (23) Yang, M.-Ch.; Ynag, T.-S.; Wong, M.-S. *Thin Solid Films* **2004**, 469/470, 1.
- (24) Ynag, T.-S.; Yang, M.-C.; Shiu, C.-B.; Chang, W.-K.; Wong, M.-S. *Appl. Surf. Sci.* **2006**, 252, 3729.
- (25) Battiston, G. A.; Gerbas, R.; Porchia, M.; Rizzo, L. *Chem. Vap. Deposition* **1999**, 5, 13.
- (26) Gracia, F.; Holgado, J. P.; González-Elipe, A. R. *Langmuir* **2004**, 20, 1688.
- (27) SRIM—The Stopping and Range of Ions in Matter. <http://www.srim.org>. As based on: Biersack, J. P.; Haggmark, L. *Nucl. Instrum. Methods* **1980**, 174, 257.
- (28) Khan, Sh.U. M.; Al-Shahry, M.; Ingler, W. B. *Science* **2002**, 297, 2243.
- (29) Justicia, I.; Ordejón, P.; Canto, G.; Mozos, J. L.; Fraxedas, J.; Battiston, G.; Gerbas, R.; Figueras, A. *Adv. Mater.* **2002**, 14, 1399.
- (30) Saha, N. C.; Tompkins, H. G. *J. Appl. Phys.* **1992**, 72, 3072.

- (31) Irie, H.; Washizuka, S.; Yoshino, N.; Hashimoto, K. *Chem. Commun.* **2003**, *11*, 1298.
- (32) Chen, X.; Burda, C. *J. Phys. Chem. B* **2004**, *108*, 15446.
- (33) Sakai, N.; Wang, R.; Fujishima, A.; Watanabe, T.; Hashimoto, K. *Langmuir* **1998**, *14*, 5918.
- (34) Wang, R.; Sakai, N.; Fujishima, A.; Watanabe, T.; Hashimoto, K. *J. Phys. Chem. B* **1999**, *103*, 2188.
- (35) Rico, V.; López, C.; Borrás, A.; Espinós, J. P.; González-Elipé, A. R. *Sol. Energy Mater. Sol. Cells* **2006**, *90*, 2944.
- (36) Lee, J.-Y.; Park, J.; Cho, J.-H. *Appl. Phys. Lett.* **2005**, *87*, 011904.
- (37) Nakamura, R.; Tanaka, T.; Nakato, Y. *J. Phys. Chem. B* **2004**, *108*, 10617.
- (38) Irie, H.; Washizuka, S.; Watanabe, Y.; Kako, T.; Hashimoto, K. *J. Electrochem. Soc.* **2005**, *152*, E351.